

Short communication

Infrared light active photocatalyst for the purification of airborne indoor pollutants



K.M.S.D.B. Kulathunga, Asangi Gannoruwa, Jayasundera Bandara *

National Institute of Fundamental Studies, Hantana Road, CP 20000 Kandy, Sri Lanka

ARTICLE INFO

Article history:

Received 19 February 2016

Received in revised form 1 July 2016

Accepted 28 July 2016

Available online 29 July 2016

Keywords:

Photocatalysis

IR photon

Low energy active photocatalyst

Airborne pollutants

Ag coated TiO₂

ABSTRACT

In photocatalysis, most of the catalysts are active either for UV or visible radiations and infrared active catalysts are rare. In this investigation, Ag₂O/Ag/TiO₂ catalyst was synthesized and successfully applied for the degradation of gaseous phenol under IR irradiation. As the photodegradation described in this report involves low energy IR photons under ambient indoor conditions, the catalytic system can be applied for the degradation of common airborne pollutants found in indoors.

© 2016 Elsevier B.V. All rights reserved.

1. Introduction

Airborne pollutants such as volatile organic compounds (VOC), hydrogen sulphide, nitrogen oxides, and carbon monoxide, can cause health problems. Among common organic pollutants, phenolic compounds are highly volatile and the VOCs are of particular concern in air pollution [1,2]. As airborne phenolic compounds have been especially recognized as carcinogenic agent for human, strict guidelines have been implemented to regulate the airborne phenolic compounds [3]. An extensive attention has been devoted to find efficient routes to destroy organic pollutant from air, water and soil. Advanced oxidative processes (AOP) have been applied successfully for the degradation of phenolic compounds.

AOP confine with chemical and physical agents such as a combination of oxidizing agents such as semiconductors/photocatalyst, hydrogen peroxide, ozone and electrochemical oxidation. In heterogeneous photocatalysis, phenolic compounds are broken down to smaller non-toxic compounds on the semiconductor materials with the assistance of UV and visible radiations [3,4]. The most widely used semiconductor photocatalyst i.e. TiO₂ is photoactive in the higher energy range of solar spectrum due to high band gap of TiO₂. Therefore, bandgap engineering is essential for the tuning of bandgap energy of TiO₂ in order to activate in lower energy radiations such as IR and visible regions of solar spectrum. Many attempts have been devoted to utilize the visible spectrum of solar energy by impurity doping, metallization and sensitization of TiO₂ [5–8]. However, catalysts that utilize the IR region which confine

over 47% of solar spectrum for the photodegradation of pollutants are rare. Finding IR and near IR active photocatalysts for the degradation of common indoor pollutants is of great interest as IR and near IR photons are the common radiations found in indoor conditions. In this study, utilization of IR region for the degradation of airborne pollutants by silver nanoparticle embedded TiO₂ photocatalyst is reported and the catalyst has great application in abatement of indoor airborne pollutants.

2. Experimental

The Ag embedded TiO₂ photocatalyst was prepared by slightly modified method which is given in our previous publications [6,9]. In brief, the catalyst was synthesized by slowly adding a stoichiometric amount of 1.0 M NH₄OH to solutions containing x mg of AgNO₃ (x = 25.0, 30.0, 35.0, 40.0, 45.0 mg, BDH, Analytical grade) and 100 mg of TiO₂ (P25, Degussa) in 5 ml of water. Vigorous stirring was maintained during addition of NH₄OH to complete hydrolysis of AgNO₃ and the suspension was heated at 120 °C until a dry powder is formed and the resulting dry product was sintered at 180 °C for 1 h. In order to compare the photocatalytic behaviour of pristine TiO₂ and AgNO₃ catalysts, the similar procedure was followed except the addition of AgNO₃ and TiO₂ respectively.

The photocatalytic reaction was carried out in a gas sealed glass tube (10 ml) in which 50 mg of catalyst was spread as a thin film on the wall of the vessel. The reaction system was sealed with a gas sealed septum, wrapped three times with Al foil to make sure a complete dark condition and 10 ml of ~200 ppm phenol gas was injected to the sealed reactor at 60 °C and irradiation was carried out with IR light source in a

* Corresponding author.

E-mail addresses: jayasundera@yahoo.com, bandaraj@ifs.ac.lk (J. Bandara).

darkroom. For uniform irradiation, 8 bulbs of IR illuminating LED (880 nm, \varnothing 5 mm, light intensity 3.2 mW cm^{-2}) were mounted around the flask. Control experiments were done using the same reactor setup separately in the presence of TiO_2 , Ag_2O and without any catalyst under IR illumination. Dark controls were carried out in the same reactor with $\text{TiO}_2/\text{Ag}_2\text{O}$, TiO_2 and Ag_2O without the IR light source. Gaseous products of the reactor system were analysed by gas chromatography (Shimadzu, GC-9AM, packed charcoal column) coupled with TCD and Ar as carrier gas. To measure CO_2 at low concentrations, a higher amount of gaseous were injected to GC and average value of five analysis were taken as a reading. For low Diffuse Reflectance Infrared Fourier Transform spectroscopy (DRIFT) measurements of the catalysts were carried out by using Thermo Nicolet 6700 FT-IR spectrometer coupled with smart iTR. Diffuse reflectance analysis and luminescence experiments were done using a Shimadzu 2450 UV-vis spectrophotometer and Shimadzu RF 5000 recording spectrofluorophotometer instruments respectively. TEM image of the catalyst is recorded by FEI Tecnai F-20, 200 kV instrument.

3. Results and discussion

In an earlier publication, we reported the characterization of the catalyst by SEM, XRD, XPS and TEM [6,9]. According to our previous results, presence of anatase and rutile forms of TiO_2 together with cubic Ag_2O , AgO and Ag^0 in the catalyst were confirmed by the X-ray diffraction analysis. Also, XPS results confirmed that the catalyst contains Ag^+ , Ag^0 , Ti^{3+} and Ti^{4+} oxidation states and hence the catalyst was labelled as $\text{Ag}_2\text{O}/\text{Ag}/\text{TiO}_2$ [6,9]. The TEM image of the $\text{Ag}_2\text{O}/\text{Ag}/\text{TiO}_2$ catalyst is shown in Fig. 1 and the magnified TEM image of the $\text{Ag}_2\text{O}/\text{TiO}_2$ catalyst is shown in Fig. S1 in SI. The presence and distribution of Ag, Ag_2O over TiO_2 can be observed in dark colour spots having two different sizes in Fig. 1, while, the light colour spots represent the TiO_2 nanoparticles. The distribution of Ag and Ag_2O particles over TiO_2 found to sporadic, however almost all TiO_2 particles are covered with Ag and Ag_2O nanoparticles. As shown in Fig. S1, the particles with fringe widths of 0.24 nm confirms the presence of Ag_2O while the particles with fringe width of 0.35 nm confirm the presence of TiO_2 anatase [101] lattice plane. The UV-vis diffuse reflectance spectrum of the $\text{Ag}_2\text{O}/\text{TiO}_2$ catalyst is shown in Fig. 2. As demonstrated earlier and shown in Fig. 2, the $\text{Ag}_2\text{O}/\text{TiO}_2$ catalyst absorbs light from UV region to near IR region due to presence of reduced Ti^{3+} states in $\text{Ag}_2\text{O}/\text{TiO}_2$ catalyst. [6,9].

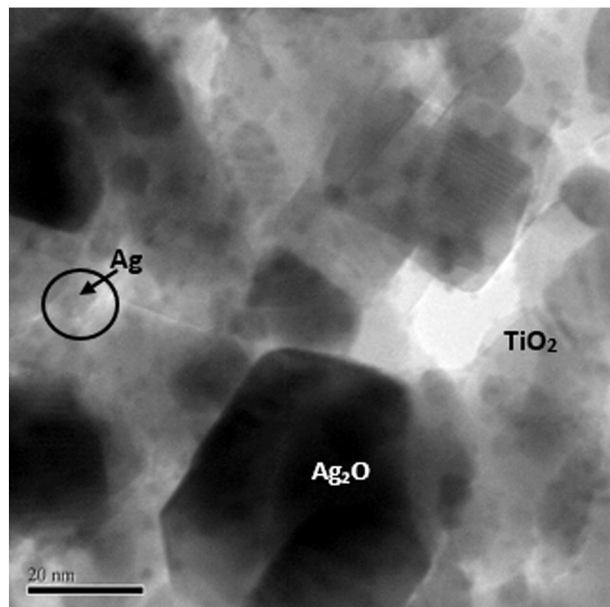


Fig. 1. TEM micrographs of $\text{Ag}_2\text{O}/\text{TiO}_2$ catalyst.

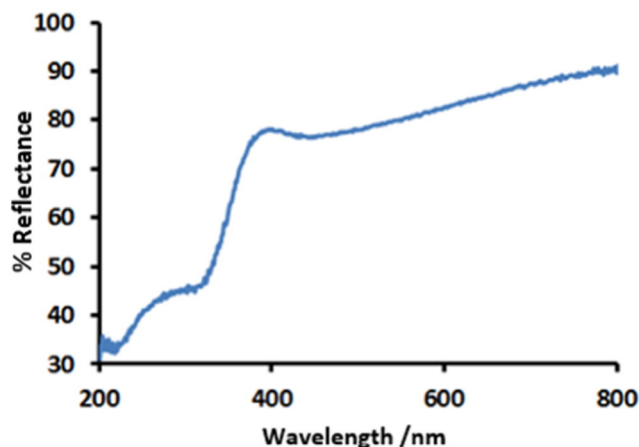


Fig. 2. Diffuse reflectance spectrum of $\text{Ag}_2\text{O}/\text{TiO}_2$ catalyst.

The CO_2 yields when the $\text{Ag}_2\text{O}/\text{Ag}/\text{TiO}_2$ catalyst with different ratios (i.e. $\text{TiO}_2:\text{AgNO}_3$ (w/w), [(A) 100:25, (B) 100:30, (C) 100:35, (D) 100:40, (E) 100:45]) were irradiated with IR photons in the presence of gaseous phenol (200 ppm) are shown in the Fig. 3. The inset in Fig. 3 shows the CO_2 yield under the same condition in the presence of TiO_2 and $\text{Ag}_2\text{O}/\text{Ag}$ alone. As shown in Fig. 3, when $\text{Ag}_2\text{O}/\text{Ag}/\text{TiO}_2$ catalyst coated reactor containing gaseous phenol were irradiated with IR photons, formation of CO_2 was clearly observed with $\text{Ag}_2\text{O}/\text{Ag}/\text{TiO}_2$ while negligible CO_2 was observed with TiO_2 and $\text{Ag}_2\text{O}/\text{Ag}$ alone. i.e. in the cases of $\text{Ag}_2\text{O}/\text{Ag}/\text{TiO}_2$ ($\text{TiO}_2/\text{Ag}_2\text{O}$ w/w ratio of 100:35), 27.70 μmol of CO_2 were observed after 2 h of irradiation while for TiO_2 and Ag_2O alone, 0.10 μmol and less than 0.10 μmol of CO_2 were observed respectively after 2 h irradiation when ~ 200 ppm gaseous phenol was irradiated with IR photons. Detectable CO_2 or any other gaseous products were not observed for dark control experiments, with $\text{Ag}/\text{Ag}_2\text{O}$ catalyst or in the absence of catalyst with IR illumination indicating that the photodegradation of gaseous phenol by $\text{Ag}_2\text{O}/\text{Ag}/\text{TiO}_2$ catalyst occurs only with IR photons. From the CO_2 yield shown in Fig. 3, it can be deduced that 21% mineralization of 200 ppm of gaseous phenol with $\text{Ag}_2\text{O}/\text{Ag}/\text{TiO}_2$ catalyst, prepared with 100:35 weight ratio of $\text{TiO}_2:\text{AgNO}_3$ in 120 min. While with TiO_2 and Ag_2O alone, a negligible amount of phenol was mineralized. As shown in Fig. 3, the degradation of phenol is highly depended on the $\text{TiO}_2:\text{Ag}_2\text{NO}_3$ ratio where increase in the $\text{TiO}_2:\text{Ag}_2\text{NO}_3$ ratio increase the degradation rate and the highest efficiency was noted when the $\text{TiO}_2:\text{Ag}_2\text{NO}_3$ ratio was 100:35 (w/w). Further increase in the ratiion resulted in decrease in the degradation

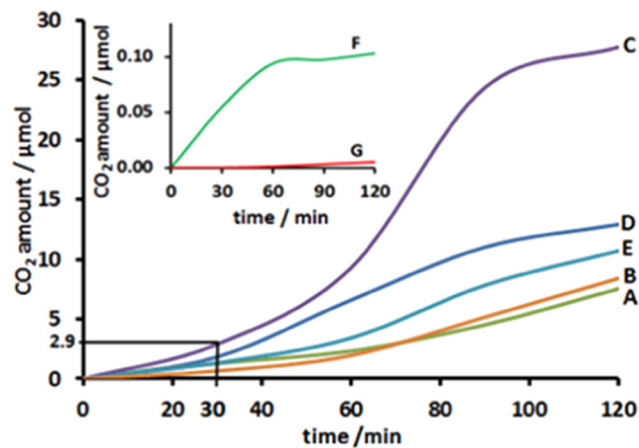


Fig. 3. Yield of CO_2 under IR irradiation in the presence of 200 ppm gaseous phenol with $\text{Ag}_2\text{O}/\text{Ag}/\text{TiO}_2$ catalyst prepared with the weight ratio of (a) 100:35, (b) 100:40, (c) 100:45, (d) 100:30, (e) 100:25 TiO_2 to AgNO_3 .

rate. The dependence of the phenol degradation with the $\text{TiO}_2:\text{Ag}_2\text{NO}_3$ ratio is given in Fig. S2 in the supporting information.

For further confirmation, that the observed degradation of phenol with $\text{Ag}_2\text{O}/\text{Ag}/\text{TiO}_2$ in the presence of IR radiation is not due to thermal activity, we investigated the thermal degradation of phenol at different temperatures without any catalyst or light. The Fig. S3 In SI shows the CO_2 yield with the reaction temperature in the presence of phenol with the $\text{Ag}_2\text{O}/\text{Ag}/\text{TiO}_2$ catalyst and without any catalyst. As shown in Fig. S3, a considerable CO_2 amount was not noted up to 80°C and from 80°C onwards, the CO_2 production is gradually increased up to 210°C and beyond this temperature a dramatic CO_2 yield is noted with the $\text{Ag}_2\text{O}/\text{Ag}/\text{TiO}_2$ catalyst while at any temperature up to 250°C , a considerable CO_2 amount was not noted in the absence of catalyst. These results indicate that phenol undergoes thermal oxidation at $\sim 250^\circ\text{C}$ yet the amount CO_2 produced under thermal degradation ($2.5\ \mu\text{mol}$ s) is much lower than the CO_2 produced under photodegradation ($30\ \mu\text{mol}$ s). These results undoubtedly confirm that the origin of observed CO_2 was due to photodegradation of gaseous phenol by $\text{Ag}_2\text{O}/\text{Ag}/\text{TiO}_2$ catalyst with IR photons and not due to thermal degradation of phenol.

The degradation results presented indicated that the degradation of gaseous phenol occurred only with $\text{Ag}_2\text{O}/\text{Ag}/\text{TiO}_2$ catalyst while both TiO_2 and Ag_2O alone showed a little or a negligible catalytic activity with IR photons. Hence, for the verification of these results, phenol adsorption and degradation on TiO_2 and $\text{Ag}_2\text{O}/\text{Ag}/\text{TiO}_2$ under IR illumination were analysed using FTIR spectroscopy and the results are shown in Fig. 4A and B respectively. In Fig. 4A, the broad peaks at about 3356 and $1642\ \text{cm}^{-1}$ correspond to the surface-adsorbed water and hydroxyl groups of TiO_2 respectively and a feeble peak at $850\ \text{cm}^{-1}$ corresponds to the Ti—O—Ti stretching vibration of Ti ions in an octahedral coordination (spectrum a in Fig. 4A) [10–14]. The spectrum A2, in Fig. 4A shows the vibrational spectra of adsorbed phenol on TiO_2 . For the adsorbed phenol on TiO_2 , where bands located at 1595 , 1499 and $1473\ \text{cm}^{-1}$ could be assigned to C=C stretching and C—H stretching vibrations [15–18]. While the band at $1368\ \text{cm}^{-1}$ corresponds to OH bending and the band located at $1239\ \text{cm}^{-1}$ is due to stretching vibrational modes of C—O in the aromatic ring [16,17]. The spectra A3, A4 and A5 in Fig. 4A show the vibrational spectra of adsorbed phenol on TiO_2 with the IR irradiation time of 30, 90, and 120 min respectively. Careful analysis of spectra A3, A4 and A5 indicates that there are no significant changes in intensity of phenol vibrations despite 0.05% mineralisation of phenol on TiO_2 . These results confirm that the TiO_2 itself is a rather inactive photocatalyst with IR irradiation.

Similarly, phenol adsorption and degradation on $\text{Ag}_2\text{O}/\text{Ag}/\text{TiO}_2$ is demonstrated in Fig. 4B. Compared to broad vibrational spectra observed for surface-adsorbed water and hydroxyl groups of bare TiO_2 , for bare $\text{Ag}_2\text{O}/\text{Ag}/\text{TiO}_2$ catalyst, four bands were observed at 3053 , 3196 , 3273 and $3356\ \text{cm}^{-1}$ which are associated with the presence of hydroxyl groups [17]. In the $\text{Ag}_2\text{O}/\text{Ag}/\text{TiO}_2$ bare catalyst, the band at $1633\ \text{cm}^{-1}$ could be assigned to both hydroxyl groups of TiO_2 (Ti—OH) and Ag—O vibrations [10,19]. Additional vibrational peaks were seen for $\text{Ag}_2\text{O}/\text{Ag}/\text{TiO}_2$ bare catalyst in the range 1500 – $1200\ \text{cm}^{-1}$ (peaks at 1431 , 1373 , 1327 and $1219\ \text{cm}^{-1}$) which are not seen in bare TiO_2 indicating those peaks are due to incorporation of $\text{Ag}_2\text{O}/\text{Ag}$ on TiO_2 and could be due to Brønsted and Lewis acid sites [20,21]. The characteristic vibrational peaks for adsorbed phenol are seen at 1585 , 1489 , $1470\ \text{cm}^{-1}$ (aromatic skeleton vibration plus C—H stretching), $1368\ \text{cm}^{-1}$ (OH bending), $1231\ \text{cm}^{-1}$ (stretching vibrational modes of C—O), 1167.5 , 1050 and $1068\ \text{cm}^{-1}$ (C—H in plane bending), 996 and $977\ \text{cm}^{-1}$ (C—H out of plane bending) [18]. As shown in spectra of B3 and B4 in Fig. 5B, upon application of IR light for 30 and 90 min respectively, a progressive loss in the intensity of the original phenol vibrational peaks could be observed and after 120 min irradiation, phenol vibrational peaks have been totally disappeared justifying that the phenol undergoes degradation with IR photons in the presence of $\text{Ag}_2\text{O}/\text{Ag}/\text{TiO}_2$ catalyst.

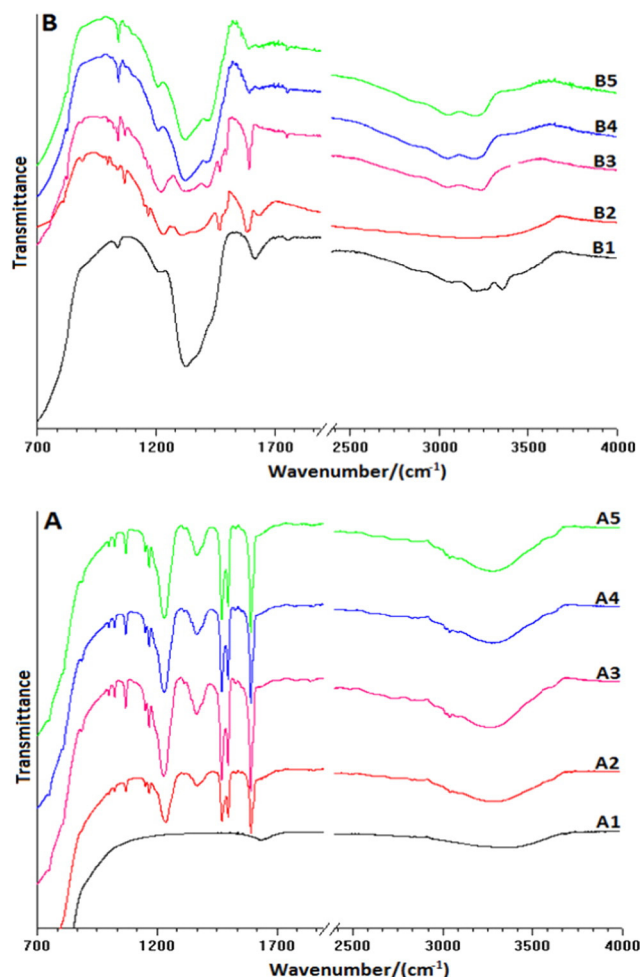


Fig. 4. (A); The FTIR transmittance spectra of 'A1' pure TiO_2 , 'A2' after dark adsorption of phenol on TiO_2 , 'A3, A4, A5' are after 30, 90 and 120 min IR illumination of adsorbed phenol on TiO_2 respectively. 4(B); The FTIR transmittance spectra of 'B1' pure catalyst, 'B2' after dark adsorption of phenol 'B3,B4,B5' are after 30, 90 and 120 min IR illumination of adsorbed phenol on TiO_2 respectively.

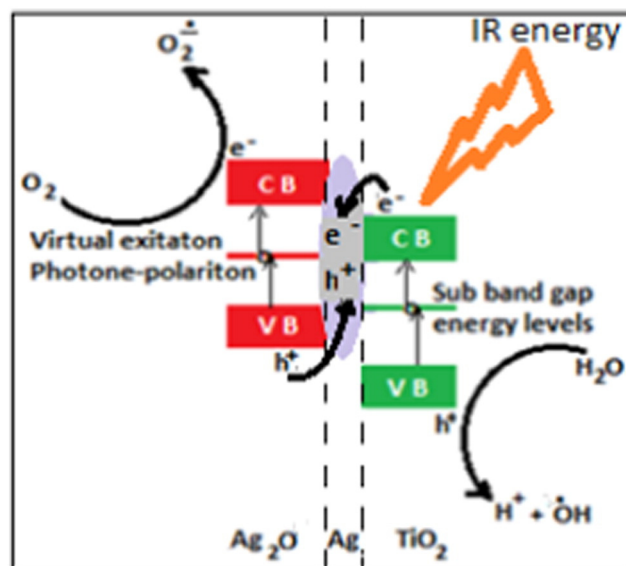


Fig. 5. Schematic diagram of proposed photocatalytic process of $\text{Ag}_2\text{O}/\text{Ag}/\text{TiO}_2$ catalyst.

Surface analysis results together with degradation results indicated the IR initiated photodegradation of phenol on $\text{Ag}_2\text{O}/\text{Ag}/\text{TiO}_2$ catalyst and phenol is mineralized producing CO_2 during degradation. Characterization of catalyst has been reported in earlier publications, where it was shown that the $\text{Ag}_2\text{O}/\text{Ag}/\text{TiO}_2$ catalyst consists of both Ag^0/Ag^+ and $\text{Ti}^{3+}/\text{Ti}^{4+}$ states in $\text{Ag}_2\text{O}/\text{Ag}/\text{TiO}_2$ catalyst. Photochemical water splitting reaction has been reported for the same catalyst and considering the excitation wavelengths of IR source (~850 and 950 nm) and the bandgap energies of TiO_2 (3.2 eV) and Ag_2O (1.58 eV)/Ag, multiphoton excitation process where optical near field (ONF) and phonon assisted reaction mechanism has been proposed and discussed in detail for the observed water splitting reaction [7].

In the proposed ONF-phonon assisted process, formation of electron hole pairs are generated via multiphoton excitation process and can be explained as follows [22] even though phonon excited states are present in semiconductors, light cannot be excited from the valence band (VB) to those phonon excited states as these excitations are electric-dipole forbidden. However, as the ONF generated at the nanostructures could excite the coherent phonon in nanoparticles and these excited coherent phonon together with ONF forms exciton-phonon-polariton quasi states as shown in Fig. 5. These quasi particles can excite the electrons to the phonon level and successively to the CB. This type of multi-step excitation process is possible even the incident photon energy is lower than the band gap energy. The generation of ONF is a pre-requisite for the proposed e-h pair generation and as explained earlier, Ag^0 and Ag_2O can generate phonons as well as ONF upon IR illumination as they are well known to generate plasmon as well as ONF [23–27].

Considering all these observations, a multiphoton process can be proposed for the observed photodegradation of gaseous phenol on $\text{Ag}_2\text{O}/\text{Ag}/\text{TiO}_2$ catalyst by IR photons where it involves filling of sub-band gaps in Ag_2O and TiO_2 by trapping and de-trapping of electrons and holes created by IR photon excitation [6,9,22]. The proposed multiphoton process is schematically shown in Fig. 5 and the possible phenol degradation paths are given in reactions (1) to (5) [9,28]. To confirm the multiphoton process, we investigated the luminescence spectrum of $\text{Ag}_2\text{O}/\text{Ag}/\text{TiO}_2$ catalyst. As shown in Fig. 6, when the $\text{Ag}_2\text{O}/\text{Ag}/\text{TiO}_2$ catalyst is excited with 650 nm wavelength, a broad emission from 350 to 500 nm range with a maximum emission at ~458 nm was observed.

As given in reactions (1) to (5), once the e-h pairs are generated by multistep processes, excited electron react with oxygen to form oxygen radical holes form hydroxyl radicals. Both these radicals can degrade phenol by the reactions given in (4) and (5).

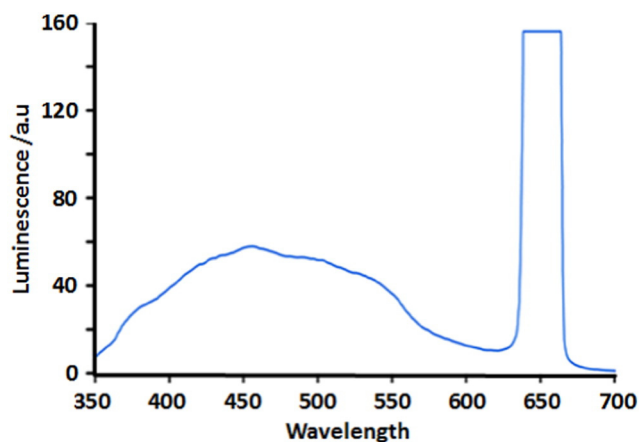
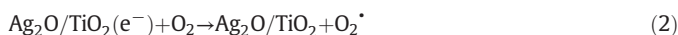
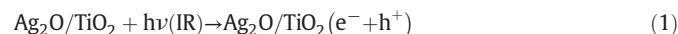
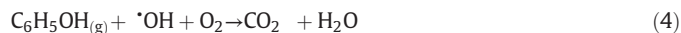
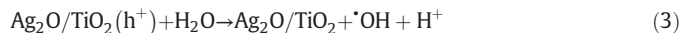


Fig. 6. Luminescence spectra of the catalyst $\text{Ag}_2\text{O}/\text{Ag}/\text{TiO}_2$ catalyst under excitation at 650 nm.



4. Conclusion

In conclusion, we have successfully demonstrated the IR initiated photodegradation of gaseous phenol on $\text{Ag}_2\text{O}/\text{Ag}/\text{TiO}_2$ catalyst. Phenol undergoes mineralization to produce CO_2 when the catalyst is irradiated with low energy IR photons. For the observed photocatalytic degradation of phenol by IR photons on $\text{Ag}_2\text{O}/\text{Ag}/\text{TiO}_2$ catalyst, a multiphoton excitation process was proposed. The $\text{Ag}_2\text{O}/\text{Ag}/\text{TiO}_2$ photoactalyst is especially useful for the abatement of airborne pollutant in indoor conditions.

Conflict of interest

The authors declare that they have no conflict of interest.

Appendix A. Supplementary data

Supplementary data to this article can be found online at <http://dx.doi.org/10.1016/j.catcom.2016.07.025>.

References

- [1] S. Scirè, S. Minicò, The role of the support in the oxidative destruction of chlorobenzene on Pt/zeolite catalysts: an FT-IR investigation, *Catal. Lett.* 91 (2003) 199–205.
- [2] F. Akhlaghian, S. Sohrabi, Fe/TiO₂ catalyst for photodegradation of phenol in water, *Int. J. Eng. Trans. A Basics* 28 (2015) 499.
- [3] M. Choquette-Labbé, W.A. Shewa, J.A. Lalman, S.R. Shanmugam, Photocatalytic degradation of phenol and phenol derivatives using a nano-TiO₂ catalyst: integrating quantitative and qualitative factors using response surface methodology, *Water* 6 (2014) 1785–1806.
- [4] S. Apollo, S. Moyo, G. Mabuoa, O. Aoyi, Solar photodegradation of methyl orange and phenol using silica supported ZnO catalyst, *Int. J. Innov. Manag. Technol.* 5 (2014) 204–205.
- [5] L. Yang, S. Luo, Y. Li, Y. Xiao, Q. Kang, Q. Cai, High efficient photocatalytic degradation of p-nitrophenol on a unique Cu₂O/TiO₂ pn heterojunction network catalyst, *Environ. Sci. Technol.* 44 (2010) 7641–7646.
- [6] A. Gannoruwa, K. Niroshan, O. Illeperuma, J. Bandara, Infrared radiation active, novel nanocomposite photocatalyst for water splitting, *Int. J. Hydrog. Energy* 39 (2014) 15411–15415.
- [7] Y. Yang, J. Wen, J. Wei, R. Xiong, J. Shi, C. Pan, Polypyrrole-decorated Ag-TiO₂ nanofibers exhibiting enhanced photocatalytic activity under visible-light illumination, *ACS Appl. Mater. Interfaces* 5 (2013) 6201–6207.
- [8] C. Yu, C.Y. Jimmy, A simple way to prepare C-N-codoped TiO₂ photocatalyst with visible-light activity, *Catal. Lett.* 129 (2009) 462–470.
- [9] A. Gannoruwa, B. Ariyasinghe, J. Bandara, The mechanism and material aspects of a novel $\text{Ag}_2\text{O}/\text{TiO}_2$ photocatalyst active in infrared radiation for water splitting, *Catal. Sci. Technol.* (2015).
- [10] A. Maira, J. Coronado, V. Augugliaro, K.L. Yeung, J. Conesa, J. Soria, Fourier transform infrared study of the performance of nanostructured TiO₂ particles for the photocatalytic oxidation of gaseous toluene, *J. Catal.* 202 (2001) 413–420.
- [11] H. Li, Z. Bian, J. Zhu, Y. Huo, H. Li, Y. Lu, Mesoporous Au/TiO₂ nanocomposites with enhanced photocatalytic activity, *J. Am. Chem. Soc.* 129 (2007) 4538–4539.
- [12] I. Villenas, B.L. Rivas, C. Torres, C. Campos, B.F. Urbano, Effect of functionalized trititanate nanotubes on the properties of crosslinked cationic polymer nanocomposite, *Polym. Int.* (2015).
- [13] S. Liu, X. Chen, A visible light response TiO₂ photocatalyst realized by cationic S-doping and its application for phenol degradation, *J. Hazard. Mater.* 152 (2008) 48–55.
- [14] A.C. Mecha, M.S. Onyango, O. Aoyi, M.N.B. Momba, Enhanced activity of metal doped titanium dioxide in photo catalytic ozonation, *Chemical Engineering & Advanced computational Technologies Pretoria (South Africa)* 2014, pp. 24–25.
- [15] R. Mendez-Roman, N. Cardona-Martínez, Relationship between the formation of surface species and catalyst deactivation during the gas-phase photocatalytic oxidation of toluene, *Catal. Today* 40 (1998) 353–365.
- [16] M.F. Atitar, H. Belhadj, R. Dilert, D.W. Bahnemann, The relevance of ATR-FTIR spectroscopy in semiconductor photocatalysis, 2015.
- [17] J. Coates, Interpretation of infrared spectra, a practical approach, *Encyclopedia of Analytical Chemistry*, 2000.
- [18] B. Ummamaheswari, R. Rajaram, High strength phenol degradation by CSMB4 at microaerophilic condition, *Int. J. Curr. Microbiol. App. Sci* 3 (2014) 847–860.

- [19] H.-T. Ren, S.-Y. Jia, Y. Wu, S.-H. Wu, T.-H. Zhang, X. Han, Improved photochemical reactivities of $\text{Ag}_2\text{O}/\text{g-C}_3\text{N}_4$ in phenol degradation under UV and visible light, *Ind. Eng. Chem. Res.* 53 (2014) 17645–17653.
- [20] N.T. Nolan, M.K. Seery, S.J. Hinder, L.F. Healy, S.C. Pillai, A systematic study of the effect of silver on the chelation of formic acid to a titanium precursor and the resulting effect on the anatase to rutile transformation of TiO_2 , *J. Phys. Chem. C* 114 (2010) 13026–13034.
- [21] J. Lu, K.M. Kosuda, R.P. Van Duyne, P.C. Stair, Surface acidity and properties of $\text{TiO}_2/\text{SiO}_2$ catalysts prepared by atomic layer deposition: UV – visible diffuse reflectance, DRIFTS, and visible Raman spectroscopy studies, *J. Phys. Chem. C* 113 (2009) 12412–12418.
- [22] T. Yatsui, T. Imoto, T. Mochizuki, K. Kitamura, T. Kawazoe, Dressed-photon-phonon (DPP)-assisted visible-and infrared-light water splitting, *Sci. Rep.* 4 (2014).
- [23] S. Linic, P. Christopher, D.B. Ingram, Plasmonic-metal nanostructures for efficient conversion of solar to chemical energy, *Nat. Mater.* 10 (2011) 911–921.
- [24] J. Tominaga, The application of silver oxide thin films to plasmon photonic devices, *J. Phys. Condens. Matter* 15 (2003) R1101.
- [25] A. Tanaka, K. Hashimoto, B. Ohtani, H. Kominami, Non-linear photocatalytic reaction induced by visible-light surface-plasmon resonance absorption of gold nanoparticles loaded on titania particles, *Chem. Commun.* 49 (2013) 3419–3421.
- [26] T. Fukaya, D. Büchel, S. Shinbori, J. Tominaga, N. Atoda, D.P. Tsai, W.C. Lin, Micro-optical nonlinearity of a silver oxide layer, *J. Appl. Phys.* 89 (2001) 6139–6144.
- [27] A.V. Kolobov, A. Rogalev, F. Wilhelm, N. Jaouen, T. Shima, J. Tominaga, Thermal decomposition of a thin AgO_x layer generating optical near-field, *Appl. Phys. Lett.* 84 (2004) 1641–1643.
- [28] M.R. Prairie, L.R. Evans, B.M. Stange, S.L. Martinez, An investigation of titanium dioxide photocatalysis for the treatment of water contaminated with metals and organic chemicals, *Environ. Sci. Technol.* 27 (1993) 1776–1782.